Published in final edited form as:
Traffic. 2009 July ; 10(7): 938–950. doi:10.1111/j.1600-0854.2009.00909.x.

High-Resolution Fractionation of Signaling Endosomes Containing Different Receptors

Gretchen McCaffrey[1,2,†], **Jonathan Welker**[1,2,†], **Jessica Scott**[1], **Louise van Der Salm**[3], and **Mark L. Grimes**[1,2,*]

[1]Division of Biological Sciences, University of Montana, Missoula, Montana, USA [2]Center for Structural and Functional Neuroscience, University of Montana, Missoula, Montana, USA [3]Institute of Molecular Biosciences, Massey University, Palmerston North, New Zealand

Abstract

Receptor endocytosis is regulated by ligand binding, and receptors may signal after endocytosis in signaling endosomes. We hypothesized that signaling endosomes containing different types of receptors may be distinct from one another and have different physical characteristics. To test this hypothesis, we developed a high-resolution organelle fractionation method based on mass and density, optimized to resolve endosomes from other organelles. Three different types of receptors undergoing ligand-induced endocytosis were localized predominately in endosomes that were resolved from one another using this method. Endosomes containing activated receptor tyrosine kinases (RTKs), TrkA and EGFR, were similar to one another. Endosomes containing $p75^{NTR}$ (in the tumor necrosis receptor superfamily) and PAC1 (a G-protein-coupled receptor) were distinct from each other and from RTK endosomes. Receptor-specific endosomes may direct the intracellular location and duration of signal transduction pathways to dictate response to signals and determine cell fate.

Keywords

endosome; nerve growth factor; organelle fractionation; receptor; signal transduction

Cell surface receptors bind ligands at the plasma membrane and initiate a myriad of signal transduction mechanisms that change gene expression and cell behavior. Endocytosis is a means of removing receptors from the plasma membrane, and this was initially thought to be a mechanism for terminating the receptor's signal; however, it is now commonly accepted that many receptors continue to signal from endosomes and can activate different effectors than those activated at the plasma membrane (1–10). Endosomes sort receptors to be recycled back to the plasma membrane or to late endosomes and lysosomes for degradation. Different receptors are endocytosed in response to ligand binding and subsequently sorted in different ways, which affects signal transduction and cell fate decisions during development (11,12).

Perhaps the most compelling rationale for receptor signaling from endosomes can be found in the developmental selection of appropriately connected neurons in the mammalian nervous system. Nerve growth factor (NGF) is secreted by the target of axonal innervation. NGF binds to its receptor, TrkA, at the axon tip of the innervating neuron and the receptors

*Correspondence: *Mark L. Grimes*, Mark.Grimes@mso.umt.edu.
††Gretchen McCaffrey and Jonathan Welker contributed equally to this work.

send survival and differentiation signals back to the cell body. 'Signaling vesicles' containing NGF and its receptor were hypothesized some time ago as the retrogradely transported signal's carrier (13,14). This paradigm is thought to apply to other neurotrophins, for example brain-derived neurotrophic factor (BDNF) and neurotrophin-3 (NT-3), which bind to TrkB and TrkC, respectively. There exists strong evidence that signaling endosomes containing an activated receptor tyrosine kinase (RTK) of the Trk family are both necessary and sufficient to convey the retrogradely transported signal in neuronal axons (15–17). This and other models for the retrograde signal's conveyance have been widely discussed (3,18–25).

Complicating the understanding of neuronal signaling pathways, there is another neurotrophin receptor, $p75^{NTR}$, which binds to all the neurotrophins. $p75^{NTR}$ is a member of the tumor necrosis factor receptor (TNFR) superfamily, and acts as a co-receptor for Trk neurotrophin receptors as well as Nogo, Lingo-1 and Sortillin (26–28). When activated by itself, $p75^{NTR}$ causes axon repulsion and apoptosis, yet these signals are reversed in the presence of activated Trk RTKs to cause axon attraction, survival, and differentiation (29–31). $p75^{NTR}$ and TrkA appear to collaborate at the plasma membrane (32–34), yet are endocytosed separately (35,36). It is not understood how Trk and $p75^{NTR}$ resolve their apparent duel with opposing signal transduction pathways when both are activated in the same cell.

The G-protein-coupled receptor (GPCR), PAC1 can also activate neurite outgrowth and cell survival, similar to the Trk RTKs, when activated by its ligand, pituitary adenylate cyclase-activating polypeptide (PACAP) (37,38). PAC1 activates the MAP kinase pathway independent of RTKs (39). In addition, PAC1 and other GPCRs may cause ligand-independent trans-activation of Trk RTKs in the Golgi complex (40,41). Activated receptors in endosomes and other intracellular membranes dictate the duration of the signal as well as the specific effectors activated. This affects the downstream pathways such as the MAP kinase pathway that functions to integrate signals to elicit an appropriate cellular response (42,43).

Given the importance of the intracellular location and duration of signaling from activated receptors for determining cell fate and pathogenesis, we were motivated to develop a high-resolution organelle fractionation technique to analyze receptors in early endosomes. Early endosomes are complex structures that appear heterogeneous by electron microscopy and may even have multiple domains within a single organelle (7,44,45). While separation of early endosomes from late endosomes has been achieved using centrifugation (46) and electrophoretic techniques (47,48), separation of different types of early endosomes has not been previously reported. We hypothesized that different receptors may be in distinct populations of endosomes after undergoing ligand-induced endocytosis. We examined early endocytic organelles containing activated receptors using mechanical permeabilization, which disrupts the plasma membrane without causing its fragmentation, allowing organelles to emerge. Plasma membrane and Golgi stay with the semi-intact cells and are removed by a low-speed centrifugation (49–52). We use this technique to show that endosomes containing activated TrkA, $p75^{NTR}$, and PAC1 are distinct from one another.

Results

We hypothesized that endosomes containing signaling receptors may be functionally distinct from canonical degradative and recycling pathways, and that they may be distinguished by mass and density. Endosomes containing NGF receptors were labeled by internalization of ^{125}I-NGF in rat pheochromocytoma (PC12) cells and separated from plasma membrane by low-speed centrifugation after mechanical permeabilization by a single passage through a

Balch homogenizer. It has previously been shown that plasma membrane and Golgi do not contaminate this organelle preparation (49,51,52). That fragments of plasma membrane do not contaminate the organelles was shown by (i) organelles that emerge from mechanically permeabilized cells were intact by electron microscopy; (ii) less than 4% of a plasma membrane protein (amyloid precursor protein) biotinylated at the cell surface was released into the organelle fractions if cells were not warmed to initiate endocytosis after biotinylation; and (iii) when cells were incubated with ^{125}I-NGF at 4°C and not subsequently warmed to initiate endocytosis, the cross-linked NGF–TrkA complex was not found in any organelles released from permeabilized cells; warming was required to detect this complex in organelles released from permeabilized cells (52).

Because endosomes containing NGF are heterogeneous in size (51), we developed a new method to separate organelles, first by size, using velocity gradient sedimentation, and then by density, using flotation equilibrium gradients (Figure 1A,B). We also developed a new method for effectively displaying the results; organelles of specific size and density can be depicted on the *z*-axis of a mass–density plot (Figure 1C). The data are more simply represented by a contour plot similar to a topographic map in which the intensity of shading indicates the height of the protein peak (Figure 1D). Neurotrophin-labeled endosomes from cultured rat (E13.5) dorsal root ganglia (DRG) neurons have similar densities to endosomes from PC12 cells (unpublished observations) as do organelles isolated directly from axons containing retrogradely transported neurotrophins (53), suggesting that PC12 cells are a suitable model for the study of neuronal membrane traffic.

Protein components of organelles fractionated in this manner were analyzed by trichloroacetic acid (TCA)-precipitating gradient fractions and performing western blots. Figure 2A shows western blots from eight velocity gradient fractions subjected to equilibrium flotation gradients. The transferrin receptor (TfR) is a marker for primary endocytic vesicles and recycling endosomes, and flotillin labels several endocytic compartments (54). Western blots were probed simultaneously with the same antibody solution and exposed for the same amount of time so that quantified data can be plotted on the same scale. For comparison, data are plotted using stacked $x-y$ plots, 3D rubber sheets (Figure S1; Supplemental Material), and mass–density plots (Figure 2B, left panels, top two rows). Lysosomes are larger and denser than recycling endosomes containing TfR, and their degree of separation is easily visualized by plotting TfR in green and lysosomes in red on the same graph (Figure 2B, top row). Similarly, flotillin's heterogeneous distribution (blue) is somewhat similar to the endoplasmic reticulum (ER, red), but flotillin organelles are less massive and less dense (Figure 2B, middle row). Endosomes containing TfR are well separated from synaptic vesicles (synaptophysin) and mitochondria (Figure 2B, bottom middle and right). Soluble proteins such as β-arrestin do not migrate into velocity gradients and do not float on equilibrium gradients and thus appear on the upper right quadrant of mass–density plots (Figure 2B, bottom left).

Having achieved separation of endosomes from other intracellular organelles, we next examined the localization of different endosomal compartments using antibodies to Rab5 (primary endocytic vesicles), Rab4 (recycling vesicles from early or sorting endosomes), and Rab7 (multivesicular carrier vesicles destined for late endosomes; Figure 3A). The distribution of these three markers overlaps but also shows differences, indicating that different endosomal compartments may be distinguished using this technique. The heterogeneous distribution of Rab7, and its partial overlap with lysosomes (Figure S2) is consistent with Rab7 being present on multivesicular endosomal carrier vesicles that mature to become late endosomes, whose mass and density approach that of lysosomes (55).

We next examined the distribution of NGF receptors. It has previously been shown that TrkA is bound to NGF and activated (tyrosine phosphorylated) in endosomes (51,52). Figure 3B (top row) shows activated TrkA, identified by antiphospho-TrkA (pTrk, red), compared to $p75^{NTR}$ (green) after PC12 cells were bound to NGF and warmed for 10 min. There is some co-fractionation between the two receptors, but their quantitative distribution into organelles separated by mass and density is distinct. In contrast, the major peak of pTrk (red) in velocity fraction 4 overlaps with that of Rab5 (green) as shown by a yellow signal (Figure 3B, second row, right). This figure illustrates the value of plotting data using our new method; a large number of data points are efficiently displayed and differences or similarities in organelles are readily apparent.

Although Rab5-positive primary endocytic vesicles were of similar size and density to both TrkA and TfR endosomes, these two receptors were rapidly sorted from one another. Immunofluorescence microscopy comparing TrkA and TfR showed that the receptors were in different endosomes after 10 min internalization with NGF (Figure S3). Only 3% of organelles at the cell periphery were stained with both TrkA and TfR (Figure S3A, B, E). Horseradish peroxidase (HRP), a fluid-phase marker, is taken up by all endosomes. In all, 97% of internalized TrkA and 93% of TfR near the cell periphery co-stained with internalized HRP (Figure S3 C, D, E), which indicates that these organelles are endosomes. Thus, Trk and TfR endosome populations are distinct, though their major fractions cannot be distinguished by mass and density.

We used magnetic bead immunoisolation to ask whether Trk-containing endosomes are intact after the fractionation procedure. A construct was made with a myc tag linked to the cytoplasmic, C-terminus of TrkA (described in Materials and Methods) so that organelles may be immunoisolated with magnetic beads coupled to anti-myc antibody. Trk-containing organelles bound to magnetic beads were visualized by electron microscopy (Figure 4). The morphology of the immunoisolated organelles was frequently tubular, rod-shaped, and multivesicular, the latter of which is indicative of endosomes. In some cases, different domains within a single endosome were observed, in which a more electron-lucent tubular extension was bound to more magnetic beads than a multivesicular domain (Figure 4, middle panels). These data show that the two-step gradient fractionation procedure isolates intact endosomes.

The PACAP receptor, PAC1, is a G-protein-coupled receptor that, like TrkA, activates neuronal differentiation and protects against programmed cell death in neurons and PC12 cells (37). This receptor was in organelles distinct from those containing activated TrkA and $p75^{NTR}$ after NGF treatment (Figure 3B, second row, left and middle). The plot of these receptors together shows that the major peaks of pTrk (red), $p75^{NTR}$ (green), and PAC1 (blue) are distinct.

Phospho-specific antibodies allow us to identify signaling endosomes containing activated TrkA (Figure 3B), however, we do not have a reagent that detects activated PAC1 or $p75^{NTR}$. We therefore used ligand-induced stimulation of endocytosis to identify endosomes containing activated receptors. In PACAP-stimulated PC12 cells, the amount of PAC1 endosomes increased fivefold (Figure 3C, left). Mass–density plots (Figure 3C middle and right) show that PAC1-labeled organelles from PACAP-stimulated PC12 cells (green) had mass and density identical to PAC1 organelles from NGF-treated cells (blue). We assume that the small number of PAC1 endosomes that form in NGF-treated cells represents background endocytosis (5,9). These data indicate that ligand-induced PAC1 endosomes are largely distinct from pTrkA endosomes.

In contrast to PAC1, $p75^{NTR}$ was found in different endosomes with and without NGF treatment. The mass–density distribution of organelles containing $p75^{NTR}$ from cells treated with PACAP or EGF are similar to one another (Figure 5A, left column) but distinct from $p75^{NTR}$ endosomes from cells treated with NGF (Figure 5A, right column); NGF-stimulated $p75^{NTR}$ endosomes (green) were not present without NGF stimulation (blue or red). Superimposition of $p75^{NTR}$ endosomes from PACAP-, EGF-, and NGF-treated cells highlights distinct NGF-induced endosomes in green (Figure 5A, bottom right). TfR, which is constitutively endocytosed, did not change under these conditions (Figure S4A). Because the NGF-induced $p75^{NTR}$ endosomes were distinct from TrkA signaling endosomes (Figure 3B, top row), and the distribution of ^{125}I-NGF reflects both TrkA and $p75^{NTR}$ endosomes, we could determine that NGF-induced $p75^{NTR}$ endosomes contained NGF (Figure S4B).

We sought to confirm these results in another cell line that expresses TrkA and $p75^{NTR}$. Figure 5B shows that neuroblastoma SY5Y cells, as in PC12 cells, also demonstrate NGF-induced stimulation of $p75^{NTR}$ endosomes (green) that were distinct from those in cells treated with EGF (red).

When cells were stimulated with EGF, signaling endosomes containing activated EGFR were detected (pEGFR, Figure 5C). Signaling endosomes containing pEGFR (green) and pTrk (red) are similar to one another in mass and density in both PC12 (Figure 5C, top row) and SY5Y cells (bottom row). Similar to PC12 cells, SY5Y cells form a population of $p75^{NTR}$ endosomes distinct from pTrkA endosomes when induced by NGF but not EGF (Figure S4C).

To confirm these results by an independent method, we asked if we could distinguish TrkA from $p75^{NTR}$ endosomes by electron microscopy in cells (Figure 6). We used magnetic microbead internalization (Figure 6, MB) and immuno-electron microscopy (IEM) to label endosomes containing TrkA and $p75^{NTR}$. After 10 min with NGF, TrkA was detected in electron-lucent endosomes, often at the edge of the endosome, or at the ends of tubules (Figure 6A, B). In contrast, $p75^{NTR}$ was usually found in organelles with uniformly higher electron density (Figure 6C). Both TrkA and $p75^{NTR}$ were found less frequently in multivesicular organelles, but even these differed from one another in appearance (Figure 6B, center; 6C, top right). These data confirm that $p75^{NTR}$ and TrkA are internalized into different endosomes: They differ in morphology as well as mass and density.

Discussion

We describe here a new method to fractionate organelles based on mass and density, which resolves endosomes from other organelles and resolves different kinds of early endosomes from one another. The new mass–density plots presented here, which are somewhat akin to multiparametric plots from flow cytometry except that organelles instead of cells are separated, facilitate interpretation and allow concise description of data. Key elements of this technique are as follows: (i) mechanical permeabilization is a gentle homogenization technique that does not fragment the plasma membrane; (ii) organelles are fractionated in a cytoplasm-like buffer and isoosmotic gradient media; (iii) at no point are organelles compressed into a pellet and re-suspended, which may disrupt organelle membranes; and (iv) quantitative data shows the relative amounts of different receptors in different organelle pools. This latter point illustrates how high-resolution organelle fractionation complements powerful imaging techniques by providing information that is difficult or impossible to obtain by microscopy. Using the method described here, proteins that have different molecular species because of alternate splicing or posttranslational modifications can be distinguished by molecular weight on western blots. For example, we identified the immature glycosylated forms of TrkA and $p75^{NTR}$, and thus localized receptors in the ER as

distinct from post-Golgi forms. Another advantage is the potential to identify by proteomics proteins in organelles that have been well resolved from one another (46,56).

This method will be useful to assess how exogenously expressed proteins are distributed in organelles. Except for the immunoisolation experiment in Figure 4, the experiments shown here were performed without overexpression of proteins, which may cause aberrant cellular distribution because of saturation of sorting machinery, or a tag, which may disrupt interactions that are required for membrane traffic. The construct of Trk with a C-terminal myc tag was in fact more heterogeneous in organelle distribution than endogenous TrkA in PC12 cells (unpublished observations), but the immunoisolated organelles did have the multivesicular morphology of endosomes; so we can conclude that intact endosomes are isolated using this procedure.

This technique revealed an interesting biological finding—that three different kinds of receptors internalize into distinct endosomes. Based on previous studies from immunofluorescence microscopy showing that TrkA and $p75^{NTR}$ are endocytosed separately (35,36), we hypothesized that endosomes containing these two receptors may have different physical characteristics. Our data shows that this is indeed the case. We also note that TrkA and $p75^{NTR}$ endosomes have different morphology by electron microscopy (Figures 4, 6).

Because PAC1 activates the Rap1 to MAP kinase pathway from intracellular organelles as does TrkA (39), and because of the possibility of trans-activation of TrkA by PAC1 in intracellular organelles (41), one might predict a common early endosomal intermediate for these two receptors. Our data show, however, that this is not the case. TrkA and PAC1 endosomes were largely distinct, though there was a minor fraction of TrkA that overlapped with PAC1 endosomes (Figure 3B). This minor fraction contained only small amounts of Rab5 (Figure 3A). PAC1 endosomes were also distinct from NGF-induced $p75^{NTR}$ endosomes (Figure 3B). Thus, a majority of ligand-stimulated endosomes containing TrkA, PAC1, and $p75^{NTR}$ differed from one another in size and density. While these receptors may meet later in downstream organelles, all of these receptors have been suggested to signal from endosomes (3,27,29–31,35,36,40,51,52,57–59). Our data imply that distinct receptor-specific signaling endosomes form shortly after receptors are activated.

The method described here complements fluorescence microscopy and other techniques to investigate mechanisms by which different receptors are sorted into a number of different endocytic pathways (60,61). One receptor may be endocytosed by more than one pathway. For example, TrkA has been shown to use both clathrin-dependent and clathrin-independent endocytosis (62,63). Similarly, GPCRs use a clathrin-independent pathway as well as clathrin-dependent endocytosis (61). Nevertheless, the major populations of endosomes containing TrkA, PAC1, and $p75^{NTR}$, each of which represent a different family of receptors, were distinguishable by mass and density (Figure 3).

Different organelles may have the same mass and density, however, as shown for TrkA and TfR endosomes (Figures 2 and 3), which are distinct by fluorescence microscopy (Figure S3). Similarly, TrkA and EGFR have been shown to be endocytosed by different pathways (64), but the two RTKs were not resolved from one another by size and density (Figure 5). No major differences in the mass–density distribution in these two receptors were noted when two cell populations were stimulated separately with EGF and NGF and organelles were mixed and applied to the same gradients, or when cells were stimulated with EGF and NGF simultaneously (unpublished data). Thus, this method may prove that two proteins are in distinct organelle populations but caution must be employed to interpret data when size and density overlap.

This technique identifies proteins that are tightly bound to organelles. Rab proteins were detected in the soluble pool (upper right quadrant of mass density plots, Figure 3A) but mostly bound to endosomes. In contrast, clathrin, EEA1, and β-arrestin dissociated from endosomes partly or completely during the equilibrium flotation gradients (Figure 2B and unpublished observations). This may prove useful to distinguish proteins bound to organelles with high affinity from those whose binding to organelles relies on low affinity interactions.

The concept of receptor-specific endosomes extends to the model of signaling endosomes (3,4,7,9,22,25,56). Receptor-specific endosomes may be specialized for intracellular signaling and thus contain signaling effectors such as APPL1 and GIPC, which are not present on organelles in the canonical recycling and degradative pathways (65–67). The presence of different signaling effectors on endosomes versus plasma membrane is an example of signal bifurcation that occurs sequentially. Receptor-specific endosomes may undergo sorting into the canonical recycling or lysosomal degradation pathways in ways different from constitutively endocytosed receptors such as the TfR or low density lipoprotein receptor (LDLR). Receptor-specific endosomes may be slower to enter the recycling or degradative pathway, which would prolong their activation, or they may be sorted to different cellular compartments. These effects on the duration and location of signal transduction pathways affect signal transduction and cell fate decisions during development, and may go awry during pathogenesis (11,12,55). The technique described here provides a new tool for further investigations into the mechanisms by which different receptors are sorted to different endosomes.

Materials and Methods

Materials

Antibodies were from Cell Signaling Technologies, Inc. except the following: RTA anti-TrkA was from Upstate Biotechnology and L. Reichardt (University of California, San Francisco); anti-APPL1 and anti-GIPC were from D. Kaplan (Hospital for Sick Children, Toronto, Canada); anti-$p75^{NTR}$ was from Covance/BabCo; anti-Rab5 from Abcam; TfR monoclonal H68.4 from Chemicon; sc11 anti-TrkA from Santa Cruz Biotechnology; anti-mouse and anti-rabbit HRP was obtained from Amersham Biosciences. Calyculin A was from Cell Signaling Technologies. μMACS microbeads covalently linked to anti-rabbit IgG anti-myc, or anti-LNGFR were provided by Miltenyi Biotech. Laboratory reagents were from Sigma, Mallinckrodt Baker, and Fluka.

^{125}I-NGF was prepared as previously described (52) except that biotinylated lactoperoxidase was used (Sigma) and removed by binding to neuravidin beads (Pierce) prior to separation of radiolabeled protein from free iodine.

PC12 cells and DRG neurons

Wild-type PC12 cells were obtained from Lloyd Greene (Columbia University) and grown on collagen-coated plates in RPMI 1640, 5% fetal calf serum, and 10% horse serum as described (68). SY5Y cells were obtained from Mark Israel (University of California, San Francisco) and grown in RPM1 1640, 10% fetal calf serum in 5% CO_2.

DRG neurons were obtained from E13.5 rat embryos. Ganglia were dissected and placed in Lebovitz's L-15 medium, washed in Earl's balanced salt solution, and dissociated by incubation in 0.05% trypsin. Cells were centrifuged and re-suspended in MEM, 10% fetal calf serum, 0.2% glucose, 2 m m_M glutamine with pen/strep. Neurons were cultured for 6 days in 5% CO_2 on polylysine/laminin in the presence of 1 n_M NGF.

Organelle fractionation

PC12 cells (typically $0.5 - 1 \times 10^9$) were harvested in PBS and washed in cold PEE (PBS/1m$_M$ EGTA/1m$_M$ EDTA), PGB (PBS/0.1% glucose/0.1% BSA) as described (51,52). Precise control of internalization time was accomplished by binding neurotrophins (1–2 nm NGF) at 4°C in PGB, washing unbound ligand in PGB so as to avoid fluid-phase endocytosis, warming in PGB to 37°C exactly 10 min, followed by a temperature-quench in ice water. For magnetic bead internalization experiments, all binding steps were performed at 4°C. 100 μg anti-TrkA (RTA, Upstate Biotechnology) was added 30 min after addition of neurotrophins, then 100 μL μMACS goat anti-rabbit microbeads (Miltyeni Biotech) were added and cells were mixed at 4°C for an additional 20 min.

Alternatively, anti-LNGFR μbeads (Miltyeni Biotech) were added 30 min after neurotrophin incubation and cells were incubated for 50 min as above. Cells were washed and then subjected to 10 min internalization at 37°C prior to fixation. For organelle fractionation, all subsequent procedures were performed on ice or at 4°C. Cells were washed in PEE, buffer B (cytoplasmic ionic composition: 38 m$_M$ each of the K^+ salts of aspartic acid, glutamic acid and gluconic acid, 20 m$_M$ MOPS pH 7.1 at 37°C, 10 m$_M$ potassium bicarbonate, 0.5 m$_M$ magnesium carbonate, 1 m$_M$ EDTA, 1 m$_M$ EGTA), and re-suspended in buffer B with 5 m$_M$ reduced glutathione (abbreviated BB+G). Cells were mechanically permeabilized by a single passage through a Balch homogenizer (51,52).

To harvest cultured DRG neurons, cold PEE was added and the cells slowly lifted from the culture dish, retracting their axons and remaining intact, and could thus be handled in suspension in a manner similar to that described above for PC12 cells. Neurons were bound to ^{125}I-NGF at 4°C, washed, warmed for 10 min at 37°C, and broken open by mechanical permeabilization in 0.1× buffer B, which caused the cells to swell (this hypo-osmotic treatment was not necessary for efficient permeabilization of PC12 cells, but improved permeabilization of neurons). The buffer was then made to 1 × BB + G as above.

Velocity and equilibrium centrifugation

Protease inhibitors (0.1 μg/mL aprotinin, chymostatin, leupeptin, and pepstatin A; 1 μg/mL 1,10 phenanthroline; 10 μg/mL bisbenzamide; and 1 m$_M$ PMSF) and phosphatase inhibitors (100 n$_M$ calyculin A, 1 m$_M$ Na_3VO_4) were added to the permeabilized cell suspension and the semi-intact cells and large membranes were removed by centrifugation at 1000 ×*g* (51,52). Gradients used iodixanol mixed with BB+G as media; continuous gradients were prepared using a two-chamber mixer. The supernatant of the 1000 ×*g* centrifugation (S1) was layered over 0–30% iodixanol gradients for experiments in which 5 or 24 velocity gradient fractions were collected (Figure 1A,C,D, and Figure 4) or 2.5–25% iodixanol gradients for experiments with 8 velocity fractions (Figures 2, 3, 5). Alternatively, the S1 was layered under equilibrium gradients after mixing with 60% iodixanol (Figure 1B). For two-dimensional separations (velocity followed by equilibrium gradients), velocity gradient fractions were collected as shown in Figure 1A, mixed with 60% iodixanol to a concentration of 32.5% or greater, and overlaid with a continuous 0–30% iodixanol/BB+G gradient and centrifuged to equilibrium (16–18 h). Refractive indices were measured using an Abbe refractometer (Bausch and Lomb) and converted to density using the formula ρ = R.I. × 3.4319–3.5851, which was determined empirically by weighing known concentrations of iodixanol in buffer B.

Western blots and data analysis

Samples from gradients were precipitated in 10% TCA. SDS-PAGE gels were run and western blotted to nylon-reinforced nitrocellulose (Schleicher and Schull) as described (69). Each equilibrium gradient of 24–25 fractions was run on one gel with cell extract control

and marker lanes, resulting in five or eight western blots (from five or eight velocity fractions submitted to flotation equilibrium gradients). All blots were incubated in the same antibody solution on the same day and exposed for the same amount of time. Blot incubations were performed in 5% nonfat dry milk, 150 mM NaCl, 50 mM Tris pH 7.7, 0.05% Tween 20, or conditions specified by the antibodies' manufacturer. Secondary anti-mouse or anti-rabbit antibodies coupled to HRP (Amersham) were used and chemiluminescent signals generated by Super Signal West Pico (Pierce). Blots were stripped of antibodies for re-probing with Restore (Pierce) or in 0.5 M NaCl, 0.2 M glycine, pH 2.8. Luminescence was measured using a cooled CCD camera in a Fuji LAS-3000 system and data were quantified using the Fuji Image Gauge software.

Three-dimensional color plots were generated from the quantified western blot data. Each three-dimensional color plot represents data collected from equilibrium gradients of all velocity fractions (i.e. 192 or data points). To determine the amount of proteins in endosomes versus in the whole cell (Figure 3C), the amount of proteins in organelle fractions was summed and divided by the sum in detergent-soluble and detergent-resistant fractions from cell ghosts (the 1000 ×*g* pellet) on the same western blots.

Software was written in OpenDX (OpenDX.org/Visualization and Imagery Solutions, Inc.) to display the data in three dimensions, where increasing amounts of protein components are represented by an increase in intensity of a single color (blue, green, or red). Plots of different colors were overlaid using ImageMagick (ImageMagick.org/ImageMagick Studio LLC). For the determination of $p75^{NTR}$ unique endosomes (Figure S4B), green plot images were subtracted (pTrk from NGF) and overlaid with p75 data plotted in red using ImageMagick, and threshold masking in the yellow channel was done in Adobe Photoshop. Results presented are representative of major points derived from a consensus of two or more experiments.

Immunofluorescence

PC12 cells were washed, harvested, and bound to NGF at 4°C as above. Cells were washed and incubated for 10 min at 37°C in the presence or absence of 10 mg/mL HRP, then chilled rapidly in ice water. Cells were washed twice in PEE, then fixed in 3% paraformaldehyde in PBS on ice 20 min. The cells were washed in PBS containing 1 mM lysine, then in PGB, and permeabilized in PBS containing 1% normal goat serum, 0.5% BSA, 0.1% saponin at room temperature for 15 min. Cells were washed and re-suspended in the above solution without saponin and incubated in primary antibodies: RTA, anti-TfR (H68.4), or fluorescein-anti-HRP. Secondary antibodies (fluorescein goat anti-mouse, rhodamine goat anti-rabbit, fluorescein goat anti-rabbit, Cappel; texas red goat anti-rabbit, Jackson Immunologicals) were incubated in suspension. Cells were washed by centrifugation at 200 ×*g* and placed in Fluoromount G. Images were taken on a Nikon Optiphot/BioRad MRC 600 confocal microscope. Grayscale images were false-colored in Adobe Photoshop according to secondary antibodies used. For quantitative comparisons of overlap of endosomal markers, 90–100 brightly stained organelles near the cell periphery were counted.

Immunoisolation

PC12 cells stably expressing myc-tagged TrkA were used for organelle fractionation and immunoisolation experiments. A construct was made containing a myc tag on the C-terminus of the TrkA's cytoplasmic tail and expressed in PC12 cells. The extracellular domain of TrkB extracellular domain was fused to the membrane-spanning and cytoplasmic portions of TrkA to allow us to distinguish activation of this receptor from endogenous TrkA in PC12 cells. The coding determinant of the TrkB extracellular domain and C-terminal myc-tagged TrkA transmembrane and intracellular domain were fused and put into

pAd-Track expression vector to obtain a rat TrkB-A chimeric receptor. To generate PC12 cells stably expressing TrkB-A receptors, two million wild-type PC12 cells were plated on poly- D-lysine-coated 10-cm tissue culture plates, and co-transfected with two expression vectors, one encoding the TrkB-A receptor and the other encoding a hygromycin-resistant gene. Thirty-six hours after transfection, hygromycin B (200 μg/mL) was included in the culture medium for selection. Ten to twelve days after selection, the remaining colonies were isolated. Colonies stably expressing TrkB-A receptors were identified based on BDNF-induced neurite outgrowth, and confirmed by western blot analysis. ^{125}I-BDNF applied to TrkB/A-myc cells was internalized into organelles of size and density similar to those described for ^{125}I-NGF (Figure 1 and data not shown).

For immunoisolation experiments, organelles were fractionated as above on velocity followed by equilibrium density gradients, except for glutathione which was omitted from the equilibrium gradient media (in buffer B for all procedures). Pools containing floating TrkA organelles with densities defined by the peaks observed on equilibrium gradients were made (1.07–1.14 g/mL from velocity fractions 2 and 3 from experiments where five velocity-gradient fractions were collected). BSA was added to 10 mg/mL. 100 μL μMACS microbeads (Miltyeni Biotech) were incubated in 5% BSA for 1 h on ice before being added to organelle pools. The equivalent of 25 μL bead suspension is added in this solution to the organelle pools for a 30 min incubation with rotation at 4°C. MACS separation columns (20 μL) are placed on the magnetic stand at 4°C and washed in buffer containing 5% BSA. The organelle-bead suspension is applied to the column and organelles are washed with 4 × 200 μL buffer and then eluted in 2 × 25 μl into the EM fixation buffer by removing the column from the magnet.

Electron microscopy

Samples were fixed in Karnovsky's solution for 24 h, then rinsed in caccodylate buffer (3 × 10 min.), centrifuged, and embedded in 1% agarose. Agar-embedded samples were post-fixed in 2% osmium tetroxide aqueous solution for 2 h followed by rinsing in caccodylate buffer (3 × 10 min). Samples were subjected to an ethanol series (35, 50, 75, 95, 100, and 100%) for 10 min each.

Samples for TEM analysis were infiltrated using resin series of (1:2) Polybed 812/ethanol at 1 h each, followed by infiltration of 100% resin for 1 h. The sample was allowed to cure in 100% Polybed 812 resin for 18 h at 60°C. The samples were trimmed and sectioned on a MT-XL ultramicrotome with a diamond knife at approximately 70 nm in thickness. The sections were captured on 200 mesh copper/rhodium grids and poststained with 2% uranyl acetate and counterstained with Reynold's lead citrate stain.

For immuno-electron microscopy, samples were infiltrated using a resin series of (1:2, 1:1, 2:1) LR White : ethanol for 1 h each. Samples were infiltrated with 100% LR White three times for 1 h each. Infiltrated samples were polymerized for 24 h at 60°C. Polymerized samples were sectioned on an RMC MT-XL Ultramicrotome with a diamond knife at 50–60 nm. Sections were collected on 200 mesh nickel grids supported with 0.25% formvar dissolved in ethylene dichloride. Sections were blocked with 5% BSA for 1 h. Grids were then transferred through 5 changes of 1% PBS. Grids were floated on a primary antibody diluted with appropriate BSA volume (1:1000, 1:20001° antibody) at 4°C for 1 h. Excess diluted 1° antibody was removed by floating grids on 5 changes of 1% PBS for 10 min durations. Grids were floated on 1:10 10-nm gold particles diluted with 1% PBS. Grids were washed 5 × 10 min of 1% PBS, floated on 1% aq. Glutaraldehyde, then rinsed in distilled water 5 × 10 min. Grids were stained in 2% aq. uranyl acetate for 30 min and rinsed through 5 changes of distilled water at 10 min durations. Grids were counterstained with Reynold's Lead Citrate for 15 min followed by rinsing through 5 changes of distilled water at 10 min

durations. Grids were dried and viewed on Hitachi H7100 TEM coupled with an AMT 1 K × 1 K digital camera system at 75 KV accelerating voltage.

Supplementary Material

Refer to Web version on PubMed Central for supplementary material.

Acknowledgments

We thank J. Hay for comments on the manuscript; J. Valetta and W.C. Mobley for NGF; M. Comb, F. Brodsky, D. Kaplan, D. Lin, and L. Reichardt for antibodies; D. Ginty and H. Ye for the TrkB-A-myc PC12 cells; B. Lonze and A. Riccio for help with DRG cultures; and S. Keefe, N. Weber, J. Wax, L. Fisher, M. Shryock, L. Magdenz, J. Olsen and O. Arowomole for technical assistance. M.G. was supported by the Whitehall Foundation, NIH R15NS061303 and COBRE NCRR Grant P20 RR015583, and New Zealand Funding from Health Research Council, Cancer Society, Neurological Foundation, Lottery Health, Lottery Science, Real Kids Trust, Palmerston North Medical Research Foundation, and Massey University. J.S. and R.P. were supported by NIH BRIN NCRR Grant PR-16455-02.

References

1. Baass PC, Di Guglielmo BM, Authier F, Posner BI, Bergeron JJ. Compartmentalized signal transduction by receptor tyrosine kinases. Trends Cell Biol. 1995; 5:465–475. [PubMed: 14732031]
2. Ceresa BP, Schmid SL. Regulation of signal transduction by endocytosis. Curr Opin Cell Biol. 2000; 12:204–210. [PubMed: 10712919]
3. Grimes ML, Miettinen HM. Receptor tyrosine kinase and G-protein coupled receptor signaling and sorting within endosomes. J Neurochem. 2003; 84:905–918. [PubMed: 12603816]
4. Hoeller D, Volarevic S, Dikic I. Compartmentalization of growth factor receptor signalling. Curr Opin Cell Biol. 2005; 17:107–111. [PubMed: 15780584]
5. McDonald PH, Lefkowitz RJ. Beta-Arrestins: new roles in regulating heptahelical receptors' functions. Cell Commun Signal. 2001; 13:683–689.
6. McPherson PS, Kay BK, Hussain NK. Signaling on the endocytic pathway. Traffic. 2001; 2:375–384. [PubMed: 11389765]
7. Miaczynska M, Pelkmans L, Zerial M. Not just a sink: endosomes in control of signal transduction. Curr Opin Cell Biol. 2004; 16:400–406. [PubMed: 15261672]
8. Polo S, Di Fiore PP. Endocytosis conducts the cell signaling orchestra. Cell. 2006; 124:897–900. [PubMed: 16530038]
9. Sorkin A, Von Zastrow M. Signal transduction and endocytosis: close encounters of many kinds. Nature Reviews Molecular Cell Biology. 2002; 3:600–614.
10. Wiley HS, Burke PM. Regulation of receptor tyrosine kinase signaling by endocytic trafficking. Traffic. 2001; 2:12–18. [PubMed: 11208164]
11. Emery G, Knoblich JA. Endosome dynamics during development. Curr Opin Cell Biol. 2006; 18:407–415. [PubMed: 16806877]
12. Piper RC, Katzmann DJ. Biogenesis and function of multivesicular bodies. Annu Rev Cell Dev Biol. 2007; 23:519–547. [PubMed: 17506697]
13. Greene LA, Shooter EM. The nerve growth factor: biochemistry, synthesis, and mechanism of action. Annu Rev Neurosci. 1980; 3:353–402. [PubMed: 6106451]
14. Halegoua S, Armstrong RC, Kremer NE. Dissecting the mode of action of a neuronal growth factor. Curr Top Microbiol Immunol. 1991; 165:119–170. [PubMed: 2032464]
15. Chao M. Retrograde transport redux. Neurochirurgie. 2003; 39:1–2.
16. Delcroix JD, Valletta J, Wu C, Hunt SJ, Kowal AS, Mobley W. NGF signaling in sensory neurons: evidence that early endosomes carry NGF retrograde signals. Neuron. 2003; 39:69–84. [PubMed: 12848933]
17. Ye H, Kuruvilla R, Zweifel L, Ginty D. Evidence in support of signaling endosome-based retrograde survival of sympathetic neurons. Neuron. 2003; 39:57–68. [PubMed: 12848932]

18. Barker PA, Hussain NK, McPherson PS. Retrograde signaling by the neurotrophins follows a well-worn trk. Trends Neurosci. 2002; 25:379–381. [PubMed: 12127743]
19. Ginty D, Segal R. Retrograde neurotrophin signaling: Trk-ing along the axon. Curr Opin Neurobiol. 2002; 12:268–274. [PubMed: 12049932]
20. Heerssen H, Segal R. Location, location, location: a spatial view of neurotrophin signal transduction. Trends Neurosci. 2002; 25:160–165. [PubMed: 11852149]
21. Howe C, Mobley W. Signaling endosome hypothesis: A cellular mechanism for long distance communication. J Neurobiol. 2004; 58:207–216. [PubMed: 14704953]
22. Ibáñez CF. Message in a bottle: long-range retrograde signaling in the nervous system. Trends Cell Biol. 2007; 17:519–528. [PubMed: 18029183]
23. Miller FD, Kaplan DR. On Trk for retrograde signaling. Neuron. 2001; 32:767–770. [PubMed: 11738023]
24. Neet KE, Campenot RB. Receptor binding, internalization, and retrograde transport of neurotrophic factors. Cell Mol Life Sci. 2001; 58:1021–1035. [PubMed: 11529495]
25. Zweifel L, Kuruvilla R, Ginty D. Functions and mechanisms of retrograde neurotrophin signalling. Nat Rev Neurosci. 2005; 6:615–625. [PubMed: 16062170]
26. Bandtlow C, Dechant G. From cell death to neuronal regeneration, effects of the p75 neurotrophin receptor depend on interactions with partner subunits. Sci STKE. 2004; 2004:e24.
27. Barker PA. $p75_{NTR}$ is positively promiscuous: novel partners and new insights. Neurochirurgie. 2004; 42:529–533.
28. Kirkbride KC, Ray BN, Blobe GC. Cell-surface co-receptors: emerging roles in signaling and human disease. Trends Biochem Sci. 2005; 30:611–621. [PubMed: 16185874]
29. Bamji SX, Majdan M, Pozniak CD, Belliveau DJ, Aloyz R, Kohn J, Causing CG, Miller FD. The p75 neurotrophin receptor mediates neuronal apoptosis and is essential for naturally occurring sympathetic neuron death. J Cell Biol. 1998; 140:911–923. [PubMed: 9472042]
30. Davies AM. Neurotrophins: neurotrophic modulation of neurite growth. Curr Biol. 2000; 10:R198–R200. [PubMed: 10712898]
31. Dechant G, Barde YA. The neurotrophin receptor p75(NTR): novel functions and implications for diseases of the nervous system. Nat Neurosci. 2002; 5:1131–1136. [PubMed: 12404007]
32. Hantzopoulos PA, Suri C, Glass DJ, Goldfarb MP, Yancopoulos GD. The low affinity NGF receptor, p75, can collaborate with each of the Trks to potentiate functional responses to the neurotrophins. Neuron. 1994; 13:187–201. [PubMed: 8043276]
33. Canossa M, Twiss JL, Verity AN, Shooter EM. p75(NGFR) and TrkA receptors collaborate to rapidly activate a p75(NGFR)-associated protein kinase. EMBO J. 1996; 15:3369–3376. [PubMed: 8698038]
34. Esposito D, Patel P, Stephens RM, Perez P, Chao MV, Kaplan DR, Hempstead BL. The cytoplasmic and transmembrane domains of the p75 and Trk A receptors regulate high affinity binding to nerve growth factor. J Biochem Mol Biol Biophys. 2001; 276:32687–32695.
35. Bronfman FC, Tcherpakov M, Jovin T, Fainzilber M. Ligand-induced internalization of the p75 neurotrophin receptor: a slow route to the signaling endosome. J Neurosci. 2003; 23:3209–3220. [PubMed: 12716928]
36. Saxena S, Howe C, Cosgaya JM, et al. Differential endocytic sorting of $p75_{NTR}$ and TrkA in response to NGF: a role for late endosomes in TrkA trafficking. Mol Cell Neurosci. 2005; 28:571–587. [PubMed: 15737746]
37. Ravni A, Bourgault S, Lebon A, et al. The neurotrophic effects of PACAP in PC12 cells: control by multiple transduction pathways. J Neurochem. 2006; 98:321–329. [PubMed: 16805827]
38. Vaudry D, Gonzalez BJ, Basille M, Yon L, Fournier A, Vaudry H. Pituitary adenylate cyclase-activating polypeptide and its receptors: from structure to functions. Pharmacol Res. 2000; 52:269–324.
39. Gerdin MJ, Eiden LE. Regulation of PC12 cell differentiation by cAMP signaling to ERK independent of PKA: do all the connections add up? Sci STKE. 2007; 2007:e15.

40. Rajagopal R, Chen ZY, Lee FS, Chao M. Transactivation of Trk neurotrophin receptors by G-protein-coupled receptor ligands occurs on intracellular membranes. Journal of Neuroscience. 2004; 24:6650–6658. [PubMed: 15282267]
41. Sorkin A. TRKing signals through the Golgi. Sci STKE. 2005; 2005:e1.
42. Corson LB, Yamanaka Y, Lai KM, Rossant J. Spatial and temporal patterns of ERK signaling during mouse embryogenesis. Development. 2003; 130:4527–4537. [PubMed: 12925581]
43. Pawson T. Dynamic control of signaling by modular adaptor proteins. Curr Opin Cell Biol. 2007; 19:112–116. [PubMed: 17317137]
44. Sonnichsen B, De Renzis S, Nielsen E, Rietdorf J, Zerial M. Distinct membrane domains on endosomes in the recycling pathway visualized by multicolor imaging of Rab4, Rab5, and Rab11. J Cell Biol. 2000; 149:901–914. [PubMed: 10811830]
45. De Renzis S, Sonnichsen B, Zerial M. Divalent Rab effectors regulate the sub-compartmental organization and sorting of early endosomes. Nat Cell Biol. 2002; 4:124–133. [PubMed: 11788822]
46. De Araùjo ME, Huber LA, Stasyk T. Isolation of endocitic organelles by density gradient centrifugation. Methods Mol Biol. 2008; 424:317–331. [PubMed: 18369872]
47. Schmid SL, Fuchs R, Male P, Mellman I. Two distinct subpopulations of endosomes involved in membrane recycling and transport to lysosomes. Cell. 1988; 52:73–83. [PubMed: 3345561]
48. Lindner R. One-step separation of endocytic organelles, Golgi/trans-Golgi network and plasma membrane by density gradient electrophoresis. Electrophoresis. 2001; 22:386–393. [PubMed: 11258743]
49. Grimes M, Kelly RB. Intermediates in the constitutive and regulated secretory pathways released in vitro from semi-intact cells. J Cell Biol. 1992; 117:539–549. [PubMed: 1572894]
50. Grimes M, Kelly RB. Sorting of chromogranin B into immature secretory granules in pheochromocytoma (PC12) cells. Ann N Y Acad Sci. 1992; 674:38–52. [PubMed: 1288369]
51. Grimes ML, Beattie E, Mobley WC. A signaling organelle containing the nerve growth factor-activated receptor tyrosine kinase, TrkA. Proc Natl Acad Sci USA. 1997; 94:9909–9914. [PubMed: 9275225]
52. Grimes ML, Zhou J, Beattie EC, Yuen EC, Hall DE, Valletta JS, Topp KS, LaVail JH, Bunnett NW, Mobley WC. Endocytosis of activated TrkA: evidence that nerve growth factor induces formation of signaling endosomes. J Neurosci. 1996; 16:7950–7964. [PubMed: 8987823]
53. Weible MW 2nd, Ozsarac N, Grimes ML, Hendry IA. Comparison of nerve terminal events in vivo effecting retrograde transport of vesicles containing neurotrophins or synaptic vesicle components. J Neurosci Res. 2004; 75:771–781. [PubMed: 14994338]
54. Glebov O, Bright N, Nichols B. Flotillin-1 defines a clathrin-independent endocytic pathway in mammalian cells. Nat Cell Biol. 2006; 8:46–54. [PubMed: 16341206]
55. Gruenberg J, Stenmark H. The biogenesis of multivesicular endosomes. Nat Rev Mol Cell Biol. 2004; 5:317–323. [PubMed: 15071556]
56. Wu C, Cui B, He L, Chen L, Mobley WC. The coming of age of axonal neurotrophin signaling endosomes. J Proteom. 2009; 15:46–55.
57. Saxena S, Bucci C, Weis J, Kruttgen A. The small GTPase Rab7 controls the endosomal trafficking and neuritogenic signaling of the nerve growth factor receptor TrkA. J Neurosci. 2005; 25:10930–10940. [PubMed: 16306406]
58. Saxena S, Howe C, Cosgaya JM, Hu M, Weis J, Krüttgen A. Differences in the surface binding and endocytosis of neurotrophins by p75NTR. Mol Cell Neurosci. 2004; 26:292–307. [PubMed: 15207854]
59. Deinhardt K, Reversi A, Berninghausen O, Hopkins C, Schiavo G. Neurotrophins redirect $p75_{NTR}$ from a clathrin-independent to a clathrin-dependent endocytic pathway coupled to axonal transport. Traffic. 2007; 8:1736–1749. [PubMed: 17897318]
60. Miaczynska M, Stenmark H. Mechanisms and functions of endocytosis. J Cell Biol. 2008; 180:7–11. [PubMed: 18195098]
61. Donaldson JG, Porat-Shliom N, Cohen LA. Clathrin-independent endocytosis: a unique platform for cell signaling and PM remodeling. Cell Signal. 2009; 21:1–6. [PubMed: 18647649]

62. Howe CL, Valletta JS, Rusnak AS, Mobley WC. NGF signaling from clathrin-coated vesicles: evidence that signaling endosomes serve as a platform for the Ras-MAPK pathway. Neuron. 2001; 32:801–814. [PubMed: 11738027]

63. Shao Y, Akmentin W, Toledo-Aral JJ, Rosenbaum J, Valdez G, Cabot JB, Hilbush BS, Halegoua S. Pincher, a pinocytic chaperone for nerve growth factor/TrkA signaling endosomes. J Cell Biol. 2002; 157:679–691. [PubMed: 12011113]

64. Valdez G, Philippidou P, Rosenbaum J, Akmentin W, Shao Y, Halegoua S. Trk-signaling endosomes are generated by Rac-dependent macroendocytosis. Proc Natl Acad Sci USA. 2007; 104:12270–12275. [PubMed: 17640889]

65. Miaczynska M, Christoforidis S, Giner A, Shevchenko A, Uttenweiler-Joseph S, Habermann B, Wilm M, Parton R, Zerial M. APPL proteins link Rab5 to nuclear signal transduction via an endosomal compartment. Cell. 2004; 116:445–456. [PubMed: 15016378]

66. Lin DC, Quevedo C, Brewer NE, Bell A, Testa JR, Grimes ML, Miller FD, Kaplan DR. APPL1 associates with TrkA and GIPC1 and is required for nerve growth factor-mediated signal transduction. Mol Cell Biol Hum Dis Ser. 2006; 26:8928–8941.

67. Varsano T, Dong MQ, Niesman I, Gacula H, Lou X, Ma T, Testa JR, Yates JR, Farquhar MG. GIPC is recruited by APPL to peripheral TrkA endosomes and regulates TrkA trafficking and signaling. Mol Cell Biol Hum Dis Ser. 2006; 26:8942–8952.

68. Greene LA, Aletta JM, Rukenstein A, Green SH. PC12 pheochromocytoma cells: culture, nerve growth factor treatment, and experimental exploitation. Methods Enzymol. 1987; 147:207–216. [PubMed: 3670084]

69. Francois F, Godinho MJ, Dragunow M, Grimes ML. A population of PC12 cells that is initiating apoptosis can be rescued by nerve growth factor. Mol Cell Neurosci. 2001; 18:347–362. [PubMed: 11640893]

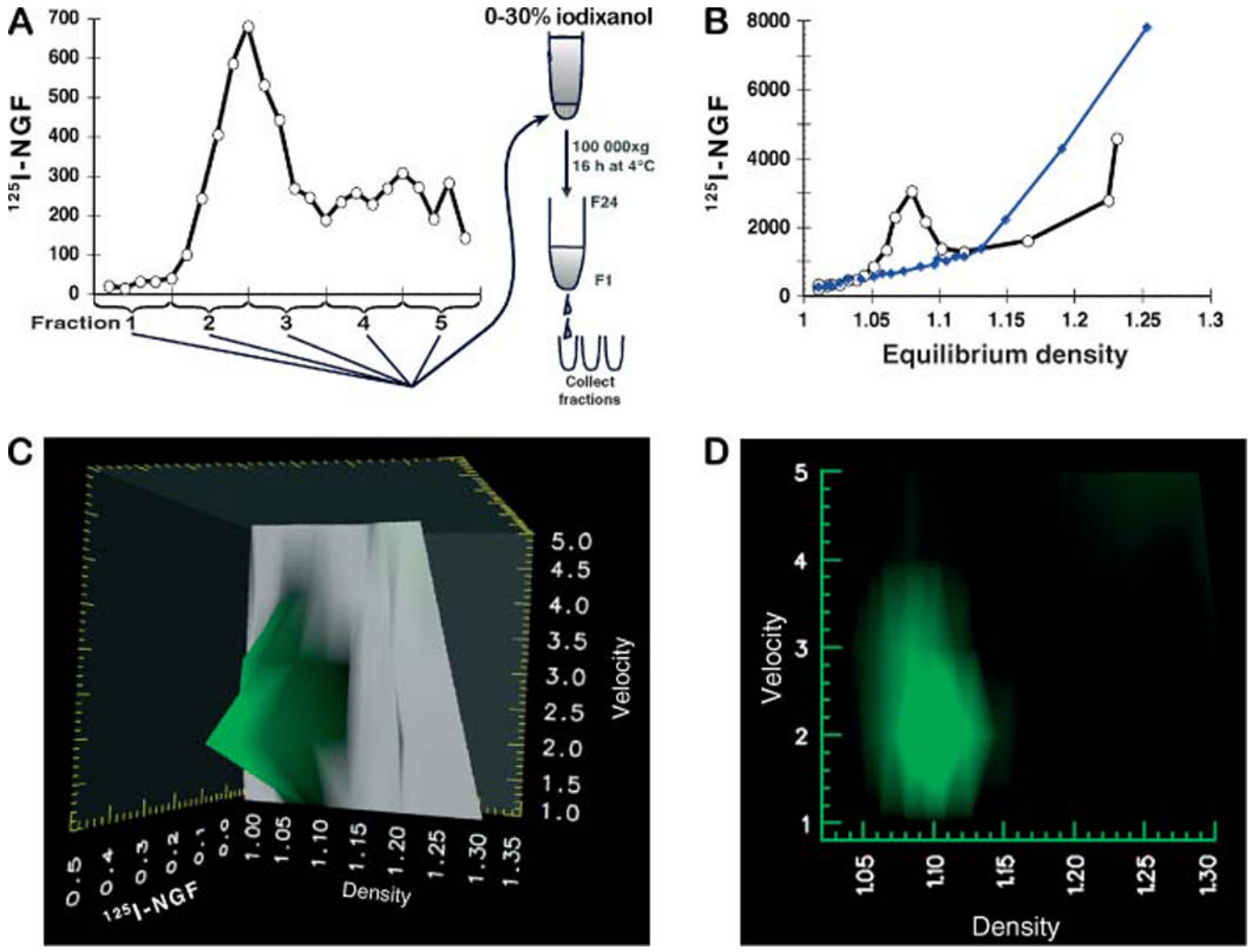

Figure 1. NGF-containing endosomes fractionated based on mass and density

A) Endosomes derived from PC12 cells after 10 min internalization of ^{125}I-NGF fractionated on an iodixanol velocity gradient. Gradient fractions were collected from the bottom, so faster-migrating (more massive) organelles are in lower numbered fractions. B) Equilibrium flotation gradients of NGF-containing endosomes as in (A) (open circles). The floating organelles (the peak at density 1.08 g/mL) were solubilized if treated with Triton X-100 prior to centrifugation (closed diamonds). For two-dimensional separations, NGF-labeled endosomes were separated first by a velocity gradient as in (A), pooled as shown, then fractions were layered under equilibrium flotation gradients as in (B). (C, D) ^{125}I-NGF data are plotted as a three-dimensional 'rubber sheet' in (C) and a color plot (as if looking down from the top) in (D).

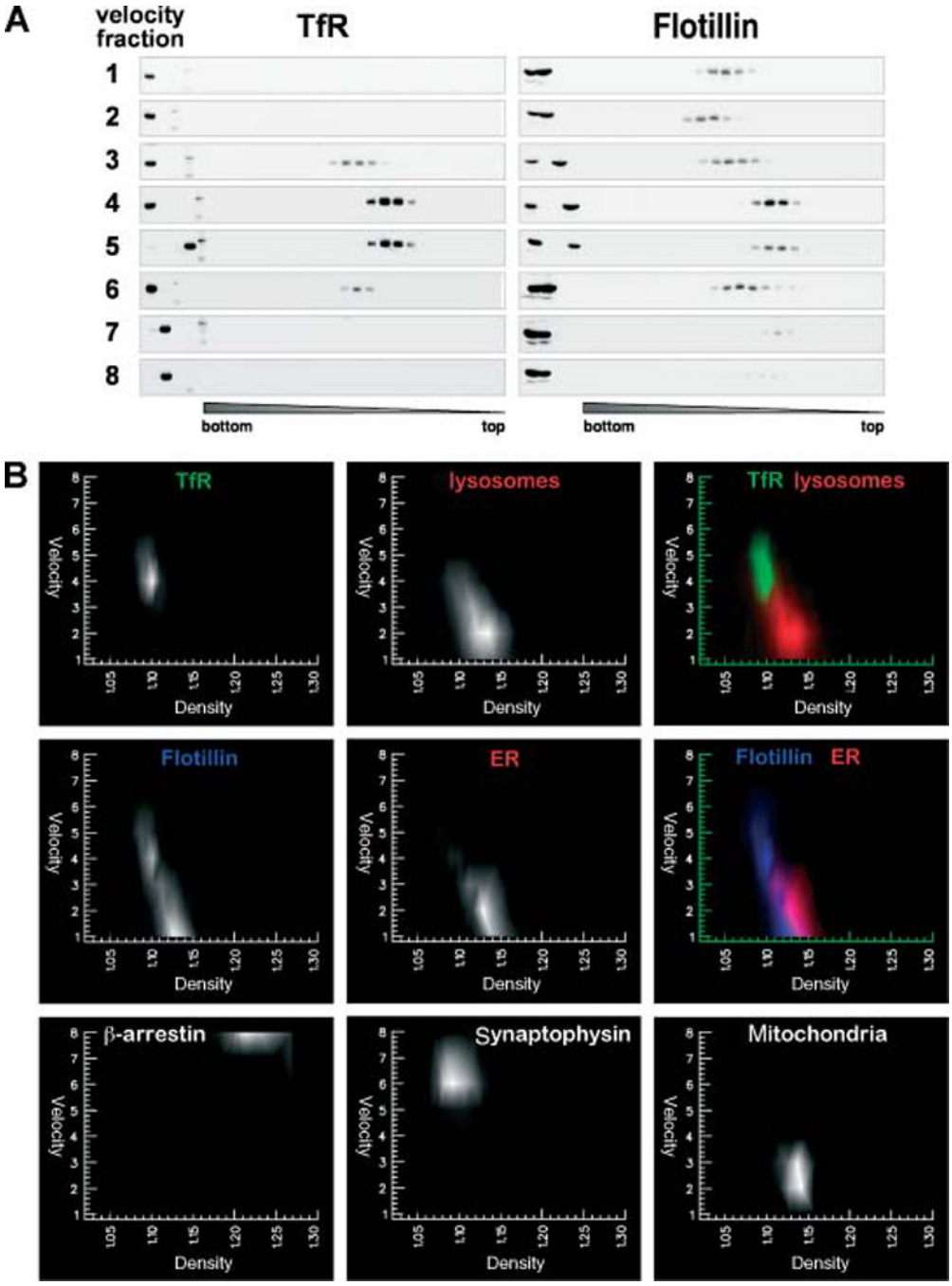

Figure 2. Mass–density fractionation of organelles

A) Western blots of flotation equilibrium gradients of velocity fractions as in Figure 1. Eight velocity gradient fractions were applied to flotation equilibrium gradients from which 24 fractions were collected. Blots were probed with anti-TfR and anti-flotillin (indicated). Detergent-soluble (P1M) and detergent-resistant (DRM) cell extracts were loaded to the left on each blot, followed by equilibrium gradient fractions 1–24 (decreasing in density from bottom to top). P1M is leftmost in velocity fractions 1–4 and 6; DRM is leftmost in 5, 7, and 8. These data were quantified and plotted in (B) (left panels). Mass–density fractionation profiles for lysosomes (acid phosphatase enzyme assay), ER (immature glycosylated TrkA), β-arrestin, synaptophysin, and mitochondria (biotinylated pyruvate carboxylase) are also

shown. To directly compare organelles, data were plotted in color and overlaid in the top right panels: TfR (green) and lysosomes (red); flotillin (blue) and ER (red). In this fractionation method, soluble, cytoplasmic protein (β-arrestin) does not enter the velocity gradient and remains at the bottom of the equilibrium gradients; synaptic vesicles (synaptophysin) have low sedimentation velocity and float on equilibrium gradients; and mitochondria and lysosomes have high sedimentation velocity and equilibrium density compared to endosomes (TfR). Flotillin, which is widely dispersed in the endocytic pathway (54), has heterogeneous size and density slightly less than ER.

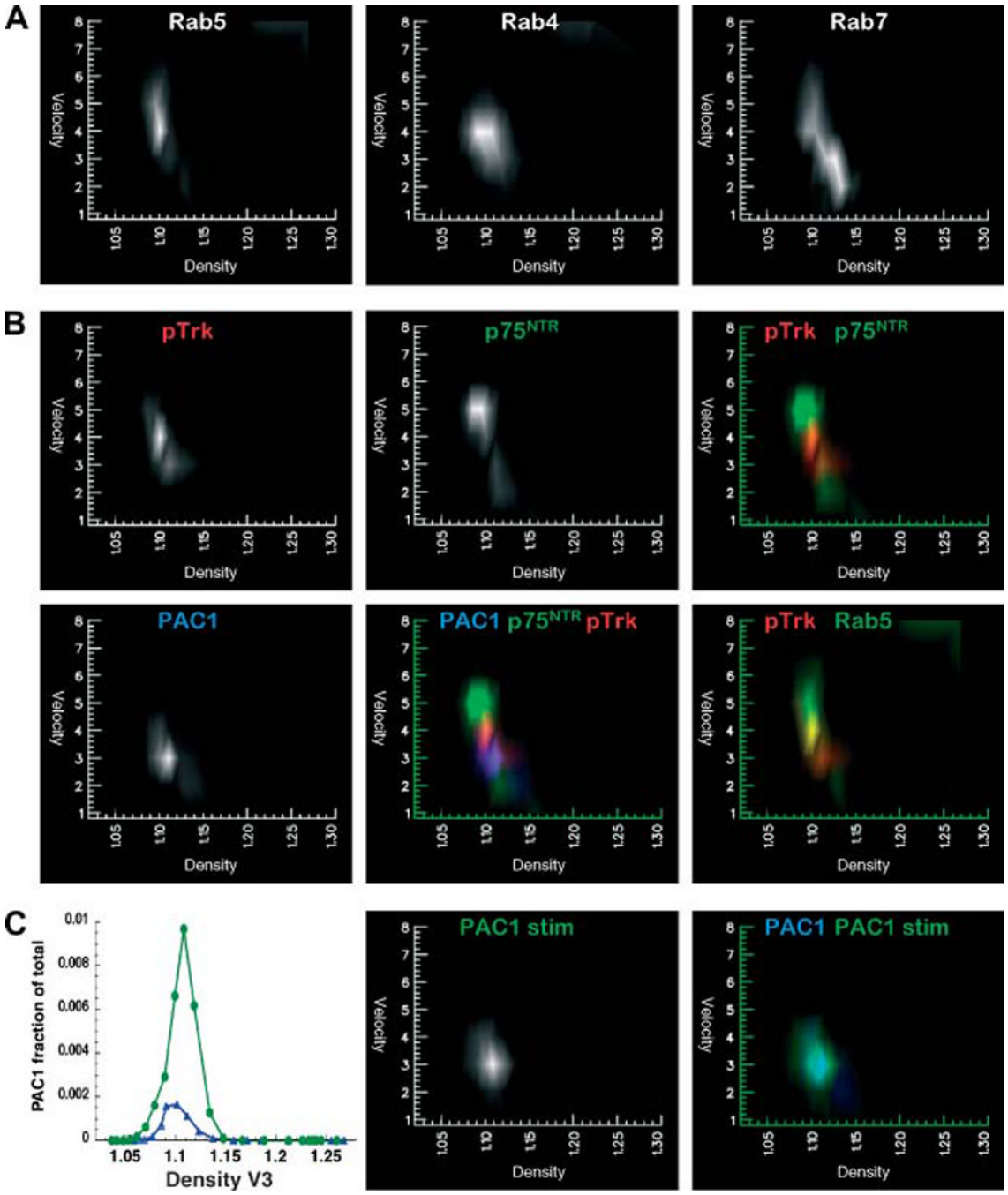

Figure 3. Resolution of receptor-specific endosomes

PC12 cells were stimulated with NGF for 10 min, endosomes were resolved by size and density, and data from western blots were quantified and plotted as in Figure 2. A) Antibodies to endosome pathway markers, Rab5, Rab4, and Rab7, identify primary endocytic vesicles, recycling vesicles destined to fuse with plasma membrane, and multivesicular carrier vesicles destined for late endosomes, respectively. B) Mass–density profiles of organelles containing NGF receptors (pTrk is phosphorylated TrkA, p75 is $p75^{NTR}$) and the PACAP receptor (PAC1) are plotted individually in white and in different colors for comparison on the same graph. The receptors, pTrk (red), $p75^{NTR}$ (green), and PAC1 (blue) largely reside in distinct endosomes (upper right and lower middle panels).

pTrk (red) overlaps with Rab5 (green) in the major peak in velocity fraction 4 (lower right panel). C) PACAP stimulation (10 min) increased the amount, but did not alter size or density of PAC1 endosomes. PAC1 amounts in velocity fraction 3 relative to the total in cells is plotted on the left panel. Mass–density profiles of PAC1 from PACAP-stimulated cells (green, circles) versus NGF-stimulated cells as in (B) (blue, triangles) is also compared on mass–density plots (right panels).

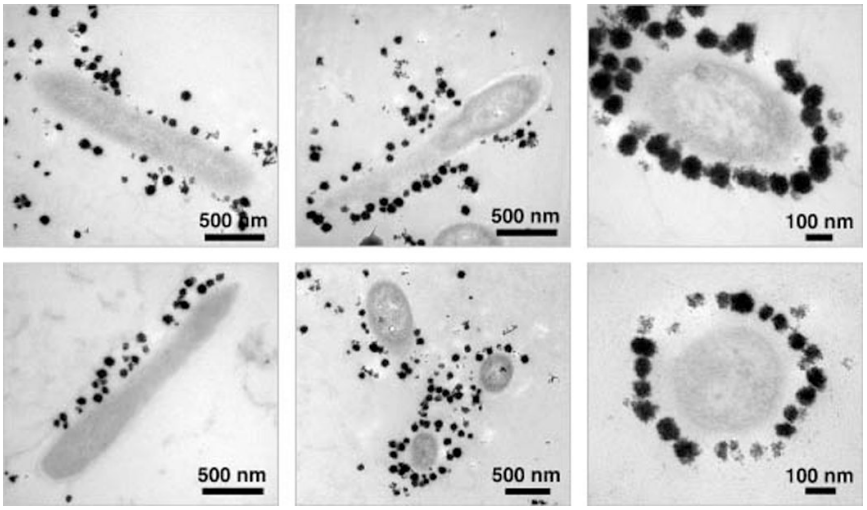

Figure 4. Electron microscopy of organelles from endosome fraction

Endosomes fractionated by size and density as in Figure 1 (C,D) were immunoisolated with magnetic beads as described in Materials and Methods. These images show organelles with Trk, myc-tagged on the cytoplasmic side of the membrane, bound to electron-dense magnetic beads (average diameter = 50 nm). Organelles with luminal vesicles were detected and in some cases, organelles with subdomains, e.g., a more electron-lucent tubular extension that appeared to bind more beads than the other, more electron-dense, multivesicular domain (middle panels).

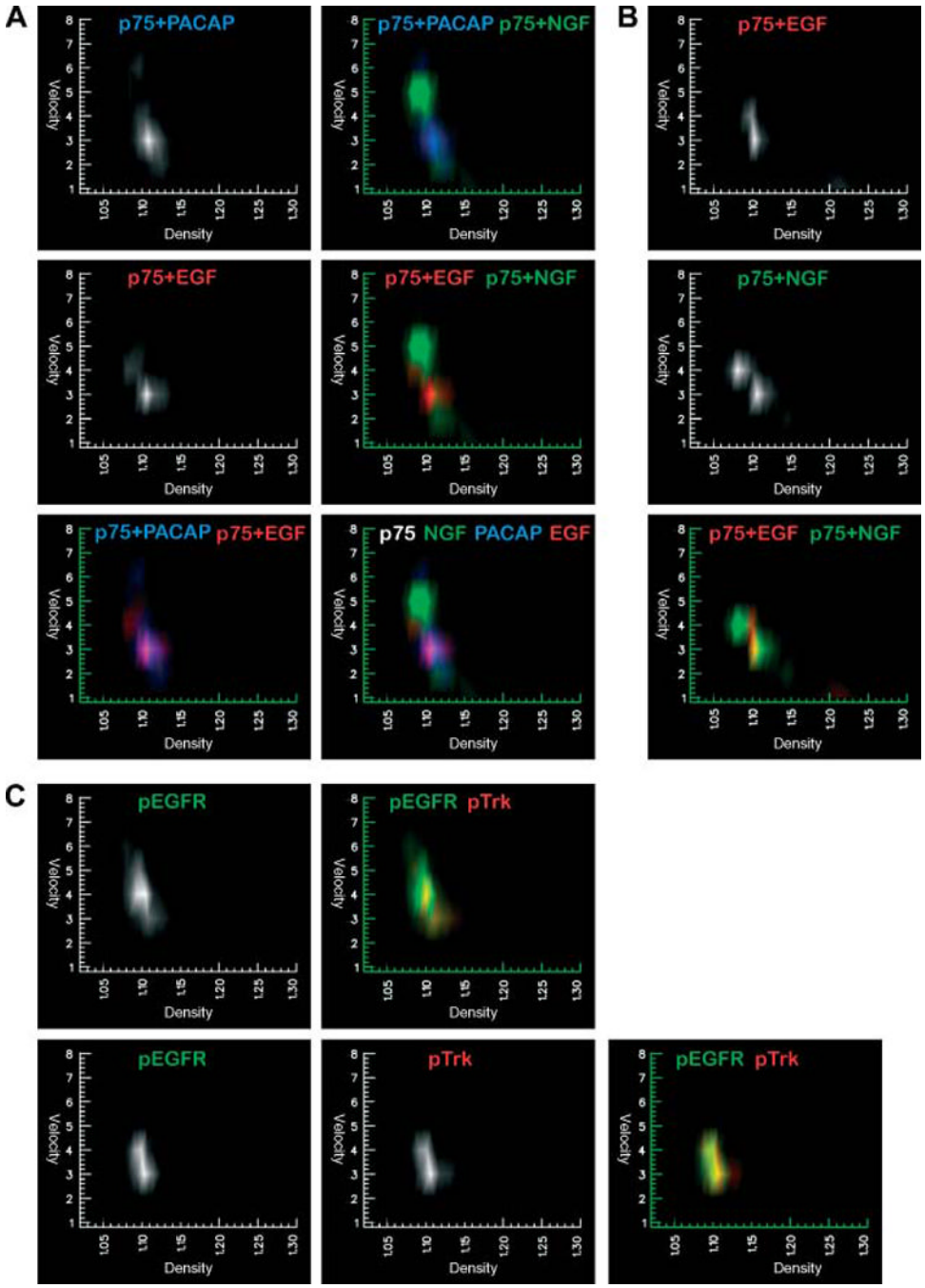

Figure 5. Stimulation of p75^{NTR} endocytosis in PC12 and SY5Y cells

A) p75^{NTR} organelles from PC12 cells stimulated with PACAP or EGF are shown in the left top and center panels. In the second column, these organelles (blue and red, respectively) are compared to p75^{NTR} organelles from cells stimulated with NGF (green; shown by itself in Figure 3B, middle). The bottom row compares p75^{NTR} organelles from PACAP- (blue) and EGF-treated cells (red) with each other (left) and with NGF-treated cells (green, right). (B, C) SY5Y neuroblastoma cells were stimulated 10 min with either EGF or NGF and the organelles containing p75^{NTR}, pEGFR, and pTrk were resolved as above. B) p75^{NTR} organelles from EGF- (top, red) and NGF-treated SY5Y cells (middle, green; overlaid on the bottom panel). As with PC12 cells, NGF stimulates formation of distinct p75^{NTR} endosomes

(green). C) RTK endosomes have similar mass–density profiles. Comparison of endosomes containing activated EGFR (pEGFR, green) and activated TrkA (pTrk, red; shown by itself in Figure 3B, top left panel) from EGF- and NGF-treated PC12 (top row) or SY5Y cells (bottom row). Signals for pEGFR and pTrkA have no background without stimulation with their respective ligands.

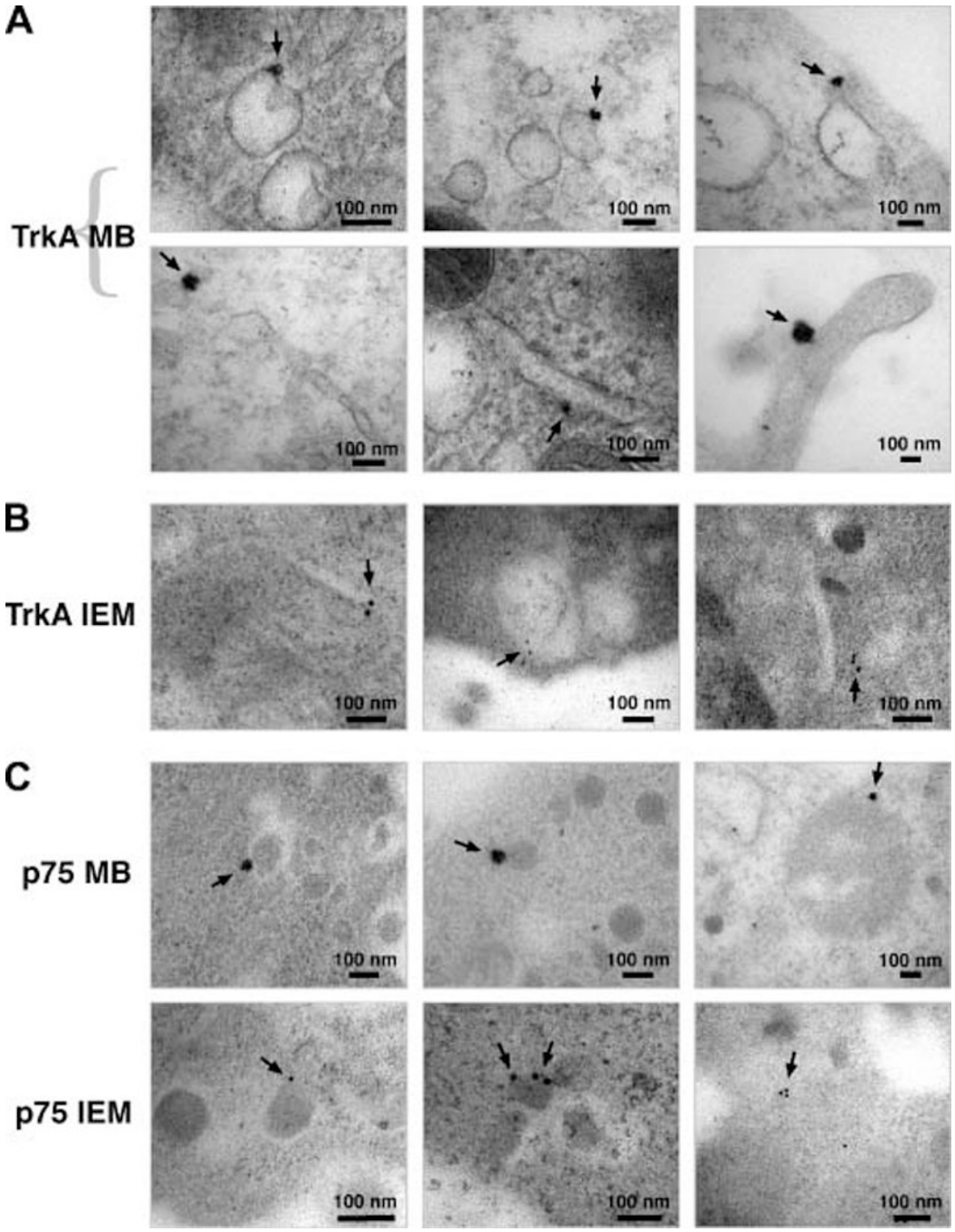

Figure 6. TrkA and p75^{NTR} are in endosomes of distinct morphology

PC12 cells were treated with NGF for 10 min. (A,C) During NGF binding and receptor internalization *in vivo*, anti-ectodomain anti-TrkA plus anti-rabbit magnetic beads (TrkA MB), or anti-p75^{NTR} magnetic beads (p75 MB) were present. Alternatively (B,C) cells were treated with NGF without antibody or magnetic beads and processed for immuno-electron microscopy (TrkA IEM); antibodies added after fixation were anti-ectodomain anti-TrkA (RTA: left and middle panels) or anti-cytoplasmic tail (SC11: right panel) or anti-p75^{NTR} (p75 IEM). Arrows point out ~ 50 nm magnetic beads or 10 nm gold particles that associate with organelles.